Chin. J. Astron. Astrophys. Vol. 1, No. 6, (2001) 514–524
(http://www.chjaa.org or http://chjaa.bao.ac.cn)

Chinese Journal of
Astronomy and
Astrophysics

Infall and Outflow Activities in the Be star FY CMa

Hui-Lai Cao ⋆

National Astronomical Observatories, Chinese Academy of Sciences, Beijing 100012
CAS-PKU Joint Beijing Astrophysics Center, Peking University, Beijing 100871

Received 2001 July 18; accepted 2001 August 28

Abstract Unusual activity of outflow mass motion connected with infall events was recorded for the B0.5 IVe star FY CMa in February 1987 from both archival *IUE* spectrograms of circumstellar N V resonance lines and optical spectra of Hα and He I λ5876 Å emission lines which showed inverse P Cygni-type profiles. We estimate the mass loss rate using ultraviolet Si IVresonance lines with expanding atmosphere modeling calculations, and describe how the radial pressure performs the dominant role in accelerating the stellar wind. We attempt to give a qualitative explanation for the activity observed for FY CMa in terms of circumstellar matter raining down to the star.

Key words: line: profiles – stars: activity – stars: emission-line, Be – circumstellar matter – stars: mass-loss – ultraviolet: stars

1 INTRODUCTION

Be stars are surrounded by an extended, low-density atmosphere or a circumstellar envelope which exhibits both differential rotation and a strong concentration to the equatorial plane of the star. Most of the circumstellar matter is in motion, some of the observed gas ultimately escapes from the star to form stellar wind. Normally, normal main sequence stars later than B0.5 are not known to exhibit mass loss phenomenon, but Be stars with emission or shell lines quite often present mass-loss behavior. The ultraviolet *IUE* (International Ultraviolet Explorer) and optical spectra of the Be star FY CMa revealed that it had experienced eruptive transient activity during early 1987.

Since 1949, the spectrum of the Be star FY CMa (HR 2855, HD 58978, MWC 179, B0.5 IVe, $v\sin i \sim 280\,\mathrm{km\ s^{-1}}$) has varied quite often. Merrill and Burwell (1949) noted that the hydrogen emission lines in the photographic region had disappeared. Burbidge and Burbidge (1954) reported that this object showed double emission lines at Nβ and Hγ with $V/R > 1$, the Balmer lines from H9 onward appeared in absorption only.

Occasional optical studies of Balmer emission line profiles obtained for this star at moderate resolution (1–2 Å at Hα) between 1981–1983 showed FY CMa to be in a rather stable state of

⋆ E-mail: caohl@bao.ac.cn

optical emission-line formation in its circumstellar disk (Dahcs et al. 1986), while a number of high-resolution *IUE* spectrograms obtained for the star since 1981 displayed strong variations in fine structure of C IV, Si IVand N V resonance absorption doublets, indicating that it undergoes a variables mass loss activity (Grady et al. 1987).

In the present work we want to draw attention to the fact that FY CMa was observed in a state of unusually high activity of mass loss variations during early 1987, as already noted by Peters (1988) and Grady et al. (1988), and that these mass-loss variation were accompanied by strong infalling motions of circumstellar matter in front of the star, simultaneously visible in the ultraviolet N V resonance absorption line profiles and in an optical He I λ5876 Å inverse P Cygni-type line profile obtained by Dachs et al. (1992).

2 DATA OBTAINED AND REDUCTION

The six high resolution ($\lambda/\delta\lambda \sim 10^4$) ultraviolet spectra obtained in 1981 (SWP 15053, 15478), 1982 (SWP 15933, 15979) and 1987 (SWP 30183, 30392) by the *IUE* spacecraft (Boggess et al. 1978) were provided by the archives of the ESA Vilspa Data Centre at the ESA Satellite Tracking Station at Villa-France del Castillo, Spain.

Two high-quality optical spectra of Hα and He I λ5876 Å were measured with the ESO Coudé Echelle Spectrometer (CES) fed by the 1.4 m Coudé Auxiliary Telescope (CAT) at La Silla, Chile. The instrumentation full width at half maximum (FWHM) measured in the thorium lamp comparison spectrum correspond to a spectral resolution of 76 mÅ at both wavelengths. These high-resolution optical spectrograms were supplemented by a total of 11 medium-resolution Hα emission line profiles obtained for the star between 1981 and 1987 by various observers of the University of Bochum at the 61-cm telescope at ESO, La Silla, using the University of Bochum scanner spectrometer at 1 ∼ 2 Å resolution, as described by Dachs et al. (1986). For both the *IUE* spectrograms and the optical spectrograms obtained at ESO, reductions were performed by means of IHAP and MIDAS image processing software systems provided by ESO. Radial velocities were first calculated in the heliocentric system, and then corrected by subtracting the radial velocities of the stars listed in the Bright Star Catalogue, $V_{\rm rad} = +25$ km s^{-1}, to obtain the velocities in the stellar reference frame. Table 1 lists the radial velocities and equivalent width of the ultraviolet spectral lines that we measured. Typical mass loss rates implied for FY CMa by the Si IVprofiles were determined with the method used by Snow (1981).

Table 1 Measurements of Lines N V–UV1, Si IV–UV1 and C IV–UV1

N V–UV1								
	λ1238.821 Å				λ1242.804 Å			
Date	$V_{\rm edge}$ (km s^{-1})	$V_{{\rm dc}(V)}$ (km s^{-1})	$V_{{\rm dc}(R)}$ (km s^{-1})	EW (Å)	$V_{\rm edge}$ (km s^{-1})	$V_{{\rm dc}(V)}$ (km s^{-1})	$V_{{\rm dc}(R)}$ (km s^{-1})	EW (Å)
81263	−698 ±22	−345 ±30	−96 ±20	1.5 ±0.1	−706 ±68	—	−100 ±18	1.3 ±0.1
81316	−812 ±73	—	−27 ±22	2.1 ±0.1	−737 ±36	−393 ±24	−54 ±28	1.9 ±0.2
82003	−637 ±46	−457 ±26	−44 ±23	0.9 ±0.2	−755 ±66	−477 ±12	−69 ±28	1.1 ±0.3
82006	−750 ±43	−448 ±36	−24 ±28	1.2 ±0.2	−773 ±60	−457 ±20	−63 ±28	1.0 ±0.2
87028	−890 ±23	−464 ±20	−32 ±22	1.8 ±0.3	−773 ±36	−450 ±28	−41 ±27	1.5 ±0.3
87057	−815 ±38	−363 ±26	+92 ±25	1.7 ±0.5	−610 ±30	−317 ±35	−60 ±20	1.3 ±0.4

Table 1 Continued

Si IV–UV1						
	λ1393.755 Å			λ1402.770 Å		
Date	FWHM	EW (Å)	$V_{\rm edge}$ (km s^{-1})	FWHM	EW (Å)	$V_{\rm edge}$ (km s^{-1})
81263	3.23 ± 0.08	3.08 ± 0.2	−950 ± 30	2.63 ± 0.08	2.08 ± 0.11	−810 ± 37
81361	3.62 ± 0.02	3.26 ± 0.3	−950 ± 40	2.25 ± 0.06	2.01 ± 0.05	−910 ± 60
82003	3.57 ± 0.11	3.45 ± 0.1	−941 ± 40	3.24 ± 0.25	3.02 ± 0.35	−990 ± 35
82006	3.37 ± 0.05	3.31 ± 0.1	−970 ± 25	2.49 ± 0.05	2.62 ± 0.05	−850 ± 40
87028	3.64 ± 0.12	3.29 ± 0.1	−940 ± 35	2.79 ± 0.05	2.51 ± 0.13	−885 ± 60
87057	3.23 ± 0.13	2.93 ± 0.2	−980 ± 50	2.88 ± 0.15	2.53 ± 0.06	−890 ± 45

C IV–UV1 λ1548.185 Å				
Date	$V_{\rm edge}$ (km s^{-1})	$V_{{\rm ma}(V)}$ (km s^{-1})	$V_{{\rm ma}(R)}$ (km s^{-1})	EW (Å)
81263	−1528 ± 56	− 59 ± 25	+205 ± 39	5.14 ± 0.2
81316	−1500 ± 74	−174 ± 33	+233 ± 22	5.71 ± 0.2
82003	−1315 ± 61	—	+169 ± 40	5.78 ± 0.3
82006	−1322 ± 124	—	+145 ± 25	5.93 ± 0.3
87028	−1396 ± 97	—	+222 ± 25	5.28 ± 0.3
87057	−1390 ± 91	−115 ± 29	+400 ± 50	4.85 ± 0.3

Notes: EW, equivalent width; $V_{\rm edge}$, edge velocity; $V_{\rm dc}$, discrete component velocity; $V_{\rm ma}$, minimum absorption component in spectrum; (V), (R), blue and red component present in line profile, respectively.

3 MORPHOLOGY OF STELLAR WIND VARIATION

Ultraviolet resonance double lines with asymmetric profile showing stellar wind absorption are inspected on six selected *IUE* spectrograms. The wavelength regions corresponding to N V (λ1235–1247 Å) and to C IV absorption (λ1539–1558 Å) are plotted in Figure 1 and Figure 2, respectively, and the Si IVdoublet region (λ1384–1412 Å) is drawn in Figure 3. The R.M. in the figures is a reseau mark which is made for wavelength calibration of the spectra. As judged from the equivalent widths and asymmetries of the C IV, N V and Si IVabsorption profiles, the stellar wind in FY CMa is very strong, in comparison with other Be stars of similar spectral types, as was noted by Grady et al. (1987). While no large variations are seen in the Si IVprofiles recorded between 1981 and 1987 (Fig. 3), dramatic variations occurred in the C IV and, even more, in the N V profiles (Fig.1). Especially the N V profiles are characterized by broad flat bottom absorption troughs in 1981 September and November, while multiple discrete absorption components located at about –30 km s^{-1} and –450 km s^{-1} dominate the N V profiles recorded both in 1982 January (day 03) and in 1987 January (day 28). By contrast, one month after 1987 January, the N V and also C IV absorption profiles taken on February 26, (day 57) are distinctly different, showing evidence for simultaneous presence of out-flowing and in-flowing motions, most probably occurring in adjacent regions of the visible circumstellar hemisphere in front of FY CMa. Outflow is observed at N V extending from about –250 km s^{-1} to at least –540 km s^{-1} and at C IV from about −175 km s^{-1} to around −1500 km s^{-1}, inflow is visible in both C IV and N V at velocities extending from 0 to about +200 km s^{-1}.

It is interesting to note that infalling motion in about the same velocity range is also clearly visible in an optical He I λ5876 Å profile of the star showing inverse P Cygni-type structure (Fig. 4), obtained on 1987 February 12 (day 43) and described earlier by Dachs et al. (1992). The sequence of the optical He I λ5876 Å profile taken 1987–43 and the ultraviolet N V λ1239 Å profile measured 1987–57 point to an extended phase of infalling motions of highly excited plasma (at electron temperature $T \geq 10^5$ K) from the circumstellar envelope of the Be star raining down to the stellar surface and lasting at least 14 days (Grady et al. 1988). In many other *IUE* spectrograms of this star, absorption by infalling matter can be detected at similar velocities ranging between +30 km s^{-1} and +100 km s^{-1} from transition of ions in lower ionization states, e.g., from Si III–UV1 λ1892.0 Å, Si III-UV4 $\lambda\lambda$1299.0, 1303.3 Å or Fe III–UV34 in λ1895.5 Å, pointing to infall of relatively cool plasma. This can be seen, e.g., 1982 January or as noted by Grady et al. (1988) in 1987 May. Terminal velocities of the expanding wind flows read from the profiles averaged around –950 km s^{-1} for the Si IVion and approximated -1450 km s^{-1} for C IV. The available medium-resolution Hα emission line profile collected between 1981 and 1987 usually indicate double-peak structure of the emission, with violet-to-red peak intensity ratios varying between $V/R \approx 1.02$ and 1.14. Equivalent width of Hα line emission recorded range between –7.3 Å measured on 1985 April 07 (R. Hanuschik, unpublished) and –14.5 Å found in 1981 November–December (Dachs et al. 1986).

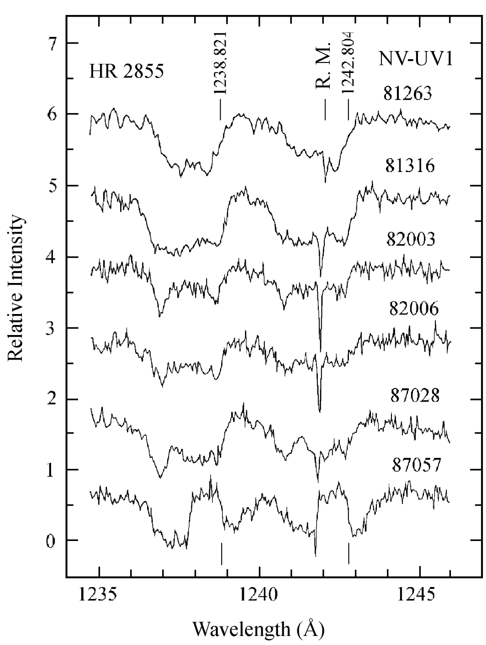

Fig. 1 Resonance Nv-UV1 doublet $\lambda\lambda$ 1238.821, 1242.840 Å wind feature showed extremely complex structure, striking emission and absorption appeared in inverse P Cygni profile.

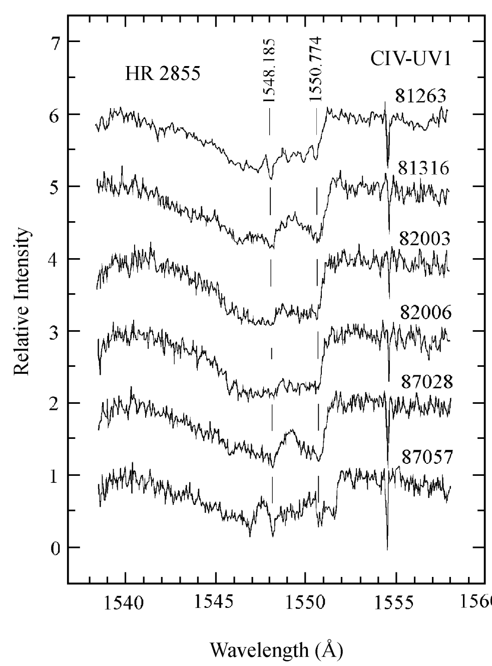

Fig. 2 Variabilities of the circumstellar resonance doublet line of Civ-UV1 $\lambda\lambda$ 1548.185, 1550.774 Å of the Be star HR 2855 during the period from 1981 to 1987. In 81263 it presented a very flate bottom absorption structure, but in 87028-87057 it showed a discrete component core.

The equivalent width of the ultraviolet spectral lines show a very good linear relation with their terminal velocities. It indicates that stellar wind plays an important role in the mass loss processing of the star (Fig. 5).

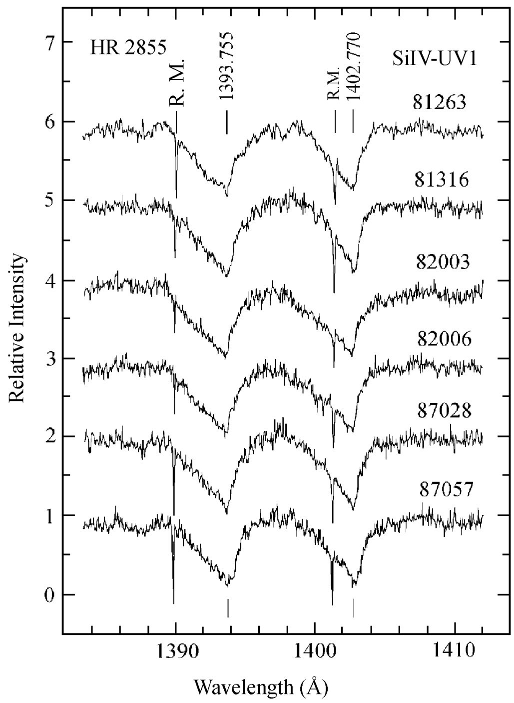

Fig. 3 Circumstellar doublet lines SiIV-UV1 1393.755 Å, 1402.770 Å in this active period have no obvious variability. The wind terminal velocity was around –900 km s^{-1}, simliar to the series hydrogen lines formed near the photosphere.

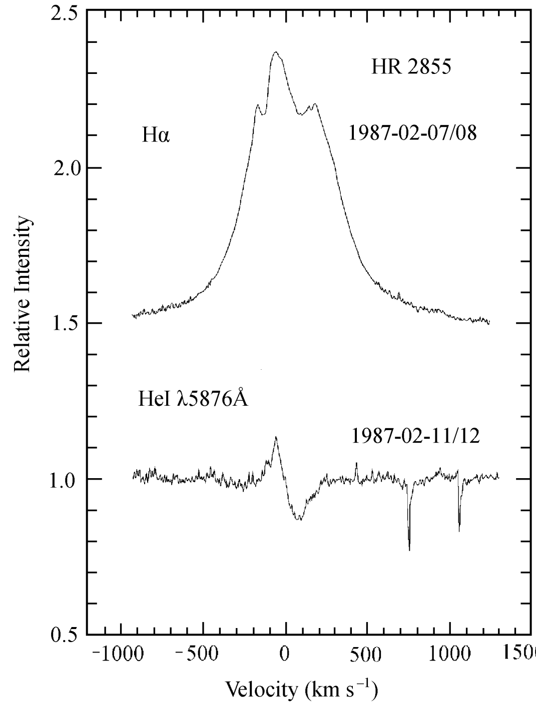

Fig. 4 Circumstellar optical line Hα and photospheric line of HeI λ 5876 Å also displayed an inverse P Cygni Profile in this active period.

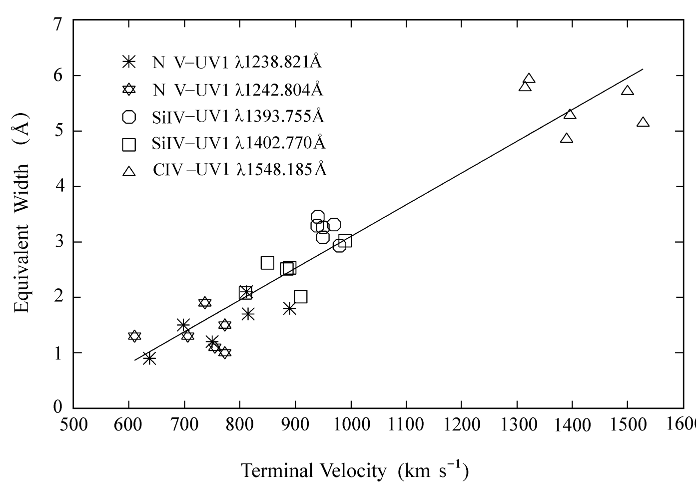

Fig. 5 Equivalent widths of the ultraviolet ions NV, SiIV, and CIV are tightly, linearly correlated with their terminal velocities.

4 MASS LOSS RATE OF THE STELLAR WIND

4.1 The Envelope Model Calculation

Spherical symmetry and a steady radial stellar wind escaping from the star are assumed, and the mass loss rate can be simply expressed as:

$$\dot{M} = 4\pi r^2 v\rho, \tag{1}$$

where ρ, v are the density and velocity of the wind, respectively, r is the wind distance from the center of the star.

If one assumes spherical symmetry and makes the Sobolev or "narrow line" approximation, the radiative transfer will become quite straightforward. The Sobolv or "narrow line" approximation is valid when the flow velocity is much larger than the ionic thermal velocity. The radial Sobolv optical depth in an expanding wind is given by Olson (1981):

$$\tau_{\rm rad}(v) = \frac{\pi e^2}{mc} f\lambda_0 \frac{R_*}{v_\infty} n_{\rm i} \left(\frac{{\rm d}v}{{\rm d}r}\right)^{-1}, \tag{2}$$

where f is the absorption oscillation strength, λ_0 (in cm) the rest wavelength, $n_{\rm i}$ (in $\rm cm^{-3}$) the number density of the absorb ions and ${\rm d}v/{\rm d}r$ (in second) the inverse velocity gradient.

The number density of ions in the lower level of the transition can be written as

$$n_{\rm i}(x) = \frac{n_{\rm i}(x)}{n_{\rm E}(x)} \frac{n_{\rm E}}{n_{\rm H}} \frac{n_{\rm H}}{\rho}\rho \equiv g(x) A_{\rm E}\mu\rho, \tag{3}$$

where $n_{\rm E}(x)$ is the number density of the observed element, $n_{\rm H}(x)$ is the number density of hydrogen, the ionization fraction $g(x) \equiv n_{\rm i}/n_{\rm E}$, element abundance $A_{\rm E} \equiv n_{\rm E}/n_{\rm H}$, and $\mu \equiv \rho/n_{\rm H}$ is the mean atomic weight per hydrogen atom.

Combining Equation (2) and Equation (3),

$$\rho = \tau_{\rm rad}(w) \Big/ \left(\frac{\pi e^2}{mc} f\lambda_0 g A_{\rm E}\mu \frac{R_*}{v_\infty}\frac{{\rm d}x}{{\rm d}w}\right) \tag{4}$$

and putting Equation (4) into Equation (1), we get the expression for the mass loss,

$$\dot{M} = \tau_{\rm rad}(w) \frac{4mc\, m_{\rm H} v_\infty^2 R_*}{e^2 f\lambda_0 g A_{\rm E}} \left(x^2 w \frac{{\rm d}v}{{\rm d}r}\right), \tag{5}$$

$\tau_{\rm rad}(w)$ can be computed from a comparison with the grid of calculated profiles with a trial combination of the parameters β, γ and T from Castor and Lamers(1979), $m_{\rm H}$ is the atomic mass of hydrogen (Snow 1981), g is the ionization fraction for the observed species, and $A_{\rm E}$, the abundance of the observed element with respect to hydrogen.

The resonance doublet line Si IV $\lambda\lambda$1393.755 and 1402.770 Å show asymmetric profiles that imply outflow stellar wind activity. The compilation of theoretical line profiles computed by Castor and Lamers (1979) are used to determine the properties of the outflowing material. Their calculations gave profile shapes as functions of a number of variables, most notably the optical depth, the velocity law and the variation of the ionization with height of the wind. The radial optical depth is specified as a function of the outflow velocity, $\tau_{\rm rad}(v)$, and the velocity law is defined as a function of the envelope distance, $v(r)$.

We normalize the distance r from the stellar center by the photospheric radius R_*, $x \equiv r/R_*$, and the velocity by the terminal velocity v_∞, $w \equiv v/v_\infty$. The model envelope is assumed to be spherically symmetric and expanding. The expanding velocity $v(r)$ increases monotonically outward and asymptotically approaches a terminal velocity, v_∞, at very large distances. We presume that the outflow velocity and optical depth in the expanding envelope vary in following ways:

(a) Velocity:

$$w(x) = w_0 + (1 - w_0)\left(1 - \frac{1}{x}\right)^\beta , \tag{6}$$

where β is a variable parameter with the values of $\beta = 0.5$, 1.0 or 4, and w_0 the assumed starting velocity at the photospheric surface, which we fix at 0.01 throughout the calculation.

(b) Optical depth:

$$\tau_{\rm rad}(w) = T(\gamma+1)(1-w_0)^{-1-\gamma}(1-w)^\gamma, \quad \gamma \geq 0 \tag{7}$$

where T is the total optical depth.

It is convenient to evaluate Equation (5) at the point in the wind where the velocity is equal to one-half of the terminal velocity. Garmany et al. (1981) showed that $\tau_{\rm rad}$ (w) evaluated at $w = 0.5$ is approximately equal to the total column-integrated line optical depth for a wide range of velocity laws and ionization profiles, one can find that $\left[x^2 w \left(\frac{{\rm d}v}{{\rm d}r}\right)\right] \approx 2.00$ and 2.04, for $\beta = 0.5$ and $\beta = 1$ at $w = 0.5$ and these values are used in Equation (5). Equation (5) will simply becomes,

$$\dot{M} = 1.74 \times 10^{-18} \tau_{\rm rad}(w)\, \frac{v_\infty^2 R_*}{f \lambda_0 g A_{\rm E}} , \tag{8}$$

where the mass loss rate $\dot{M}$ is given in units of $M_\odot\,{\rm yr}^{-1}$and the solar mass $M_\odot$ is taken as 1.9891013×10^{33} grams.

4.2 Fitting Procedure And Modeling For Determining $\dot{M}$

The Si IVresonance doublet lines display asymmetric absorption line profiles that indicate the existence of outflow, leading to a systematic velocity of the material in the stellar wind, amounting to around –980 km $\rm s^{-1}$ (Table 1). The resonance Si IVline is used to estimate the mass loss rate of FY CMa. In most of the ultraviolet resonance lines observed in the spectra of early type Be stars, the envelope profiles are superimposed onto a photospheric absorption profile. Accordingly it is necessary to allow for the photospheric contribution in the observed profiles. In principle, the true interplay between photospheric and envelope lines is more complicated, but we can simplify it according to the procedure outlined by Castor and Lamers (1979), which requires knowledge of the shape of the underlying photospheric profile. In this paper we use the long-wavelength side of the observed profile folded over to the short-wavelength side, because in an optical thin wind, the long-wavelength side of a photometric line profile is virtually unaffected by wind. The underlying photospheric profiles of Si IVare plotted in Figure 6. From the observed line profiles we can separate the resulting envelope line profiles of Si IV λ1393.755 Å and Si IV λ1402.770 Å which are respectively shown in Figure 7.

The theory for computing line profiles for photo-excited levels is explained by Castor & Lamers (1979) and Olson (1981). They computed and gave several theoretical profiles for various combinations of γ and β. For each combination, profiles are given for a range of values of the total optical depth T. We use the grid of calculation profiles to match that of the observed wind line to obtain a trial combination of β, γ and the total optical depth T, which are listed in Table 2. The stellar parameters are chosen as follows.

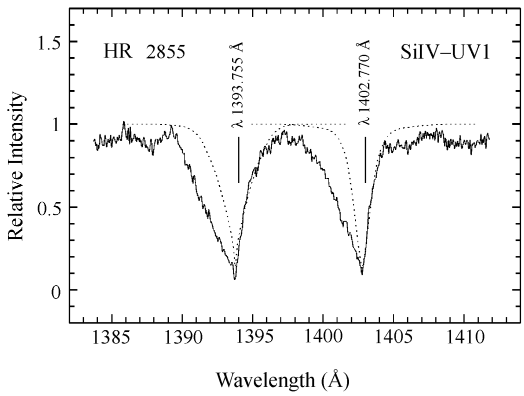

Fig. 6 Solid line is the observed doublet resonance lines of SiIV of HR 2855. Dotted line is the adopted photospheric line obtained by folding the long-wavelength side over to the short-wavelength side.

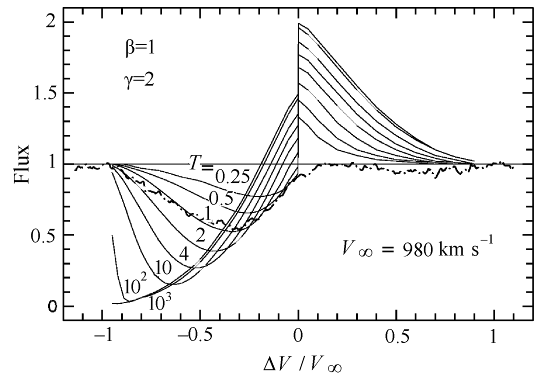

Fig. 7 Using Castor and Lamers' theoretical line profiles to match the envelope line profile derived from observed line which reduced the photospheric line profile of resonance doublet SiIV line. *Solid lines*: the theoretical line, *dash-dot line*: the envelope line.

4.2.1 Stellar Parameters

The spectral type of FY CMa is B05IV, the radius is taken as 6.5 $R_\odot$, this is obtained by interpolating from Schmidt-Kaler's (1982) table, the abundance of $N_{\rm Si\,IV}/N_{\rm H\,I} = 3.5 \times 10^{-5}$ was accepted from Kamp (1978), approximately solar abundance, the f–value is 0.528 for λ1393.755 Å and 0.262 for λ1402.770 Å, respectively (Snow 1981). We do not know the effective temperature of the radiation field seen by the ion in FY CMa's wind, but after the analysis and calculation of the triple line FeIII-UV1 $\lambda\lambda$1895.456, 1914.056 and 1926.304 Å, we determine the excitation temperature to be about 18 000 K. As we know, the excitation temperature is generally about 0.5 $\sim$ 0.6 times the effective temperature, so the effective temperature is taken to be about 35 000 K.

4.2.2 Ionization Fraction

The ionization fraction is more difficult to determine for UV lines, as noted by Drew (1989). Groenewegen et al. (1991) and Lamers et al. (1999) calculated and plotted the ionization fraction of N V, Si IVand C IV for hot stars as a function of effective temperature. From Fig. 3 in Lamers et al. (1999), for $T_{\rm eff} = 32\,000$ K, we adopt log g (Si IV) = –2.52 by interpolated estimation, then g (Si IV) = 0.003.

4.2.3 Terminal Velocity

Assuming that the lines are formed in outflowing material, the edge velocity, $v_{\rm edge}$, of the absorption wing represents a lower limit to the terminal velocity of the wind, v_∞, (Cossinelli & Abbott 1981). The edge velocity measured refers to the point where the short-ward edge of the strongest absorption profile meets the continuum. In all cases, C IV gives the largest edge velocity than that of any other lines, so the edge velocity of the line C IV is used as the terminal velocity of the wind v_∞, as listed in Table 2.

Substituting the parameters above into Equation (5), we estimate the mass loss rate $\dot{M}$ of FY CMa from the envelope line profiles of Si IV λ1393.755 Å and Si IV λ1402.770 Å to be about 3.04 $\times 10^{-7} M_\odot\,\mathrm{yr}^{-1}$and 4.28 $\times 10^{-7} M_\odot\,\mathrm{yr}^{-1}$, respectively, and list them in Table 2, this would be regarded as the mass loss rate if the wind is spherically symmetric.

Table 2 Atomic Data of Ion Si IVand Stellar Parameters

Ion Si IV (Å)	Abundance (H=1.0)	f-Value	β	γ	T	$\tau(w)$	v_∞ (km s^{-1})	$\dot{M}$ ($M_\odot\,\mathrm{yr}^{-1}$)
1393.755	3.5×10^{-5}	0.528	0.5	1	1.05	1.07	980	3.04×10^{-7}
1402.770	3.5×10^{-5}	0.262	1	2	0.85	0.65	950	4.28×10^{-7}

5 DISCUSSION

5.1 The Stellar Wind Driven Mechanism

The determination of mass loss rate in early type stars is significant for understanding both the physical origin of the mass loss and the evolution of massive stars. The presence of mass loss is strongly correlated with projected rotational velocity $v \sin i$. This shows that the mass outflow occurs primarily in the equatorial plane, or it may indicate that the mass loss is catalyzed by rapid rotation effects, since a reduction in the effective gravity near the equator due to rotation would enhance the domination of radial pressure.

We assume a toroidal, fan-shape morphology for the wind instead of spherical symmetric expanding envelope (Hummel 2000), thus $\dot{M}$ is reduced by the factor $\Omega_\mathrm{w}/4\pi$, where Ω_w is the solid angle into which the wind flows. If the concentration of the wind extends $\sim 30°$ on both sides of the equatorial plane, the total width is about 60°. The average mass loss rate, averaged over the two lines, is $\dot{M} \approx 6\times10^{-8} M_\odot\ \mathrm{yr}^{-1}$, or $\dot{M} \approx 3.8\times10^{18}$ gm s^{-1}. The terminal velocity v_∞ is taken as 980 km s^{-1}, the momentum rate of the wind, $\dot{M}\ v_\infty$, is $\sim 5.8\times10^{26}$ ($\Omega_\mathrm{w}/0.3\pi$) erg cm^{-1}. The momentum rate of the radiation, L/c, expressed empirically, is 1×10^{23} $(L/L_\odot)$ erg cm^{-1}. If we take the luminosity of FY CMa as $\sim 3.4\times10^4 \mathrm{L}_\odot$ from Schmidt-Kaler's (1982) table, the momentum of radiation is about 3.4×10^{27} erg cm^{-1}. The ratio of the radiation momentum to the wind momentum is much larger than unity. Thus radiation pressure may be sufficient to account for the observed wind. This implies the wind is driven mainly by radiation pressure.

The edge velocity represents a lower limit to the terminal velocity of the wind, v_∞. Even if the edge velocity detected from Si IVis about 980 km s^{-1}, it already greatly exceeds the escape velocity of the underlying star, $v_\mathrm{esc} = (2GM/R)^{1/2} \approx 750$ km s^{-1}, so indicating that the wind could emanate from close to surface of the star. If the wind momentum exceeds the radiation momentum, then a source of mechanical energy (e.g., rotation or magnetic field) may be required to start the wind. Abbott argued that radiation pressure in Be stars could be sufficient to drive a strong stellar wind (1982), Lucy and Solomon (1970) noted that the phenomenon is self-amplifying in that radiation absorbed by the line transfers momentum from the photons to the ions, resulting in an outward velocity which shifts the effective absorption energy to shorter wavelengths in the continuum, where the ions can be further accelerated.

Radiation pressure is believed to be the driving mechanism for the wind in many Be stars. If the acceleration due to the radiation from the central star and inner disk exceeds gravity, the wind can be accelerated to high velocities (Grady et al. 1987).

5.2 A Plausible Explanation of Simultaneous Outflow and Infall of Material

The ultraviolet and optical observations clearly show that an abrupt change in the circumstellar region around FY CMa involves the simultaneous presence of both infall and outflow of material (Peters 1988). The data which we collected show that this transient high-mass flow activity lasted for at least 30 days during the first quarter of 1987. Combining our observation with Peters' data it can be estimated that this activity persisted for more than three months. The mass loss rate is about two orders of magnitude larger than the typical stellar wind mass loss rates of many Be stars (Snow 1981). Similar, sudden spectral variations have been seen in pre-main-sequence objects in which accretion of matter is occurring (McCluskey 1988), but such bursts of activity have rarely been observed in classical Be stars.

A more plausible explanation of the abrupt activity is probably a sudden accretion event in the circumstellar envelope; as evidence, the infall of matter is clearly seen in several species of moderate ionization. Such spectral changes could be due to magnetic activity, i.e. magnetic flares or loops, FY CMa perhaps has large magnetic loops or a jet with a flow of material that originated near the pole but fell down upon the star in the line of sight. In this case the line profile presents a strong blue shift with an inverse P Cygnis feature (Baade 1989).

Acknowledgements This work was performed under the auspices of Max-Planck Society of Germany and the National Natural Science Foundation of China under the grant No.19973007. I wish to thank Dr. W. Hummel who kindly provided his observed spectra of He I and Hα obtained at La Silla, Chile, to make possible the nearly simultaneous optical observations. It is a pleasure to acknowledge helpful discussions with Prof. Dachs during my stay at Bochum University, Germany.

References

Abbott D. C., 1982, ApJ, 259, 282
Baade D., Dachs J., Weygaert R. van de Steeman F., 1988, A&A, 198, 211
Boggess A., Carr F. A., Evans D. C. et al., 1978, Nature, 275, 372
Burbidge E. M., Burbidge G. R., 1954, ApJ, 119, 496
Castor J. I., Abbott D. C., Klein R. I., 1975, ApJ, 195, 157
Cassinelli J. P., Abbott D. C., 1981, In NASA. Goddard Space Flight Center, The Universe at Ultraviolet Wavelengths The First Two Yrs. of Intern. Ultraviolet Explorer p.127
Castor J. I., Lamers H. J. G. L. M., 1979, ApJS, 39, 481
Cassinelli J. P., Olson G. L., Stalio R., 1978, ApJ, 220, 573
Cordova F. A., Mason K. O., 1982, ApJ, 260, 716
Dachs J., Hanuschik R., Kaiser D. et al., 1986, A&AS, 63, 87
Dachs J., Hummel W., Hanuschik R. W., 1992, A&AS, 95, 437
Drew J. E., 1989, ApJS, 71, 267
Garmany C. D., Olson G. L., van Steenberg M. E. et al., 1981, ApJ, 250, 660
Geoenewegen M. A. T., Lamers H. J. G. L. M., 1991, A&A, 243, 429
Ghosh K. K., Krishnamurthy R., Manivannan P. et. al., 1995, Bull. Astron. Soc. India, 23, 448
Grady C. A., Bjorkman K. S., Snow T. P., 1987, ApJ, 320, 376

Grady C. A., Peters G. J., Bjorkman K. S., et al., 1988, In ESA, A Decade of UV Astronomy with the *IUE* Satellite, Volume 1, 257
Hanuschik R. W., Dachs J., Baudzus M. et al., 1993, A&A, 274, 356
Merrill P. W., Burwell C. G., 1949, ApJ, 110, 387
Hummel W., Vrancken M., 2000, A&A, 359, 1075
Klein R. I., Castor J. I., 1978, ApJ, 220, 902
Kamp L. W., 1978, ApJS, 36, 143
Lamers H. J. G. L. M., Haser S., de Koter A., Leitherer C., 1999, ApJ, 516, 872
Lucy L. B., Solomon P. M., 1970, ApJ, 159, 879
McCluskey G. E., Kondo Y., Olson E. C., 1988, ApJ, 332, 1019
Olson G. L., 1981, ApJ, 245, 1054
Peters G. J., 1988, ApJ, 331, L33
Patterson J., 1984, ApJS, 54, 443
Schmidt-Kaller Th., 1982, in Landolt-Börnstein, NS Group VI, Vol.2, Astronomy and Astrophysics, Stars and Star Clusters, Heidelberg: Springer-Verlag, 449
Snow T. P., 1976, ApJ, 203, L87
Snow T. P., 1981, ApJ, 251, 139